

Cell Segmentation Using a Charged Active Contour

A thesis

submitted by

Olusola Akapo

In partial fulfillment of the requirements

for the degree of

Master of Science

in

Electrical Engineering

TUFTS UNIVERSITY

May 2008

Adviser: Eric Miller

ABSTRACT

In image processing, deformable models known as active contours have been used extensively to locate object boundaries in images. In this thesis, we combine concepts from two active contour methods, energy-minimizing snake active contours and charged active contours based on electrostatics to segment cells in images of human epidermal cell cultures. The first method uses energy minimization and forces computed from the gradient of an image to deform a contour so that it conforms to the boundary of an object the contour is placed in proximity to. The second method accomplishes the same task by using forces based on charged particle dynamics. We will show that by using the energy minimization model from the snake active contour and forces based on charged particle dynamics that we are able to segment the nucleus and cell wall of human epidermal cells.

ACKNOWLEDGMENTS

THANK APPROPRIATE INDIVIDUALS.

TABLE OF CONTENTS

ABSTRACT	II
ACKNOWLEDGMENTS.....	III
TABLE OF CONTENTS	IV
LIST OF FIGURES	V
CELL SEGMENTATION USING A CHARGED ACTIVE CONTOUR.....	1
CHAPTER 1: INTRODUCTION	2
1.1 INTRODUCTION	3
1.2 RESEARCH FOCUS.....	4
CHAPTER 2: TRADITIONAL SEGMENTATION METHODS	8
2.1 IMAGE PROCESSING BASICS	9
2.2 GRADIENT	10
2.3 THRESHOLDING	12
2.4 CANNY OPERATOR	14
CHAPTER 3: MATHEMATICAL BACKGROUD.....	16
3.1 INTRODUCTION	17
3.2 SNAKE ACTIVE CONTOUR	18
3.2.1 INTERNAL ENERGY AND FORCE.....	21
3.2.2 EXTERNAL ENERGY AND FORCE.....	21
3.3 CHARGED ACTIVE CONTOUR.....	22
3.3.1 BOUNDARY ATTRACTION FORCE FIELD	22
3.3.2 BOUNDARY COMPETITION FORCE FIELD	24
3.3.3 JOINT ELECTROSTATIC FORCE.....	26
CHAPTER 4: IMPLEMENTING ACTIVE CONTOURS.....	27
4.1 IMPLEMENTATION OF SNAKE ACTIVE CONTOUR	28
4.2 COMBINED SNAKE AND CHARGED ACTIVE CONTOUR	31
4.2.1 SEGMENTING THE NADH CELL IMAGES	31
CHAPTER 5: RESULTS	33
CHAPTER 6: CONCLUSION	37
REFERENCES	39

LIST OF FIGURES

FIGURE 1: HORIZONTAL GRADIENT MASK.....	11
FIGURE 2: VERTICAL GRADIENT MASK.....	11
FIGURE 3: TEST IMAGE 1	11
FIGURE 4: GRADIENT IMAGE OF TEST IMAGE 1 - OBTAINED USING EQN. 2.2.....	11
FIGURE 5: ZOOM ON VECTOR FIELD PRODUCES BY TAKING THE GRADIENT OF FIGURE 3	11
FIGURE 6: TEST IMAGE 2	13
FIGURE 7: HISTOGRAM OF TEST IMAGE 2	13
FIGURE 8: TEST IMAGE 2 AFTER THRESHOLDING WITH $T = 75$	14
FIGURE 9: TEST IMAGE 2 AFTER THRESHOLDING WITH $T = 150$	14
FIGURE 10: RESULT OF CANNY OPERATOR APPLIED TO TEST IMAGE 2	15
FIGURE 11: PARAMETRIC CURVE WITH CONTROL POINTS $V(s) = (x(s), y(s))$	18
FIGURE 12: SNAKE WITH $N=6$ VERTICES	29
FIGURE 13: RESULT 1	34
FIGURE 14: RESULT 2	34
FIGURE 15: RESULT 3	35
FIGURE 16: RESULT 4.....	35
FIGURE 17: RESULT 5	35
FIGURE 18: RESULT 5	36
FIGURE 19: SNAKE PROGRESSION	36

Cell Segmentation Using a Charged Active Contour

CHAPTER 1: INTRODUCTION



1.1 Introduction

In 2007, the American Cancer Society estimated that 559,650 people will die in the United States of cancer in that year alone. This amounts to more than 1,500 people per day [1]. On a positive note, studies show that the five year relative survival rate for all cancers diagnosed has increased to 66% (1996-2000) from 51% (1975-1977). This increase in survival rates is attributed in part to the progress made in detecting certain cancers at an earlier stage.

In order to improve detection at an earlier stage of cancer, as part of their work, the Optical Diagnostics for Diseased and Engineered Tissues (ODDET) group at the Tufts BME department has been working on developing novel optical methods to non-invasively detect precancerous lesions. The group's work has centered on the epithelium, a cell layer lining organs, where most cancers develop. The group is investigating the presence of light scattering and florescence signals that change when normal epithelial cells become transfected with human papillomavirus (HPV) or when they undergo processes that signal the onset of cancer [2].

During the course of their research, experiments using cell cultures are performed. These experiments require that cells be monitored over time to observe their development. Therefore images of the cells are taken. One of the first steps in the monitoring process is segmenting the cells. While this can be done manually, the process can be time consuming, it is difficult to reproduce results and the results are dependent on the individual who performed the

segmentation. The focus of this thesis is to develop a tool that automatically segments the cells with as little human interaction as possible.

1.2 Research Focus

Segmentation is the process of subdividing an image into its constituent regions or objects. There are the traditional model-free segmentation methods such as edge detection and thresholding that are based on the discontinuity (edge based) and similarity (region based) of pixels in an image [3]. These methods make use of local image information to segment an image and are relatively simple. However, automating them is quite difficult as they require considerable expert-user interaction due to the complexity and variability of shapes of objects of interest in an image [4]. In addition, due to image artifacts such as noise which cause the boundaries of image structures to be indistinguishable, these methods tend to just highlight the edges in an image as opposed to segmenting the image. As a result, these methods usually require some sort of post processing to clean up the segmented image. The main drawback of these methods is that the edges they find do not necessarily correspond to object boundaries within an image. Unless one is working with “nice” images that have objects with very distinct boundaries, these methods tend to produce segmented images with gaps in boundaries and phantom edges.

In the last two decades, model-based segmentation methods known as deformable models have been greatly studied. This is due to the fact that these methods have the ability to segment, match and track image structures using

constraints derived from the image [4]. In addition, these methods can make use of *a priori* knowledge about the location and shape of objects in an image in the segmentation process. This basically means that the method allows users or higher level processes to use their knowledge about the location of objects in an image to guide the segmentation process.

One such deformable model, developed by Kass et al in 1988, known as snake active contour models practically set the stage for all future work that was done (and is still being done) in the field of deformable models for segmentation. The name “active contour” basically means we are dealing with a contour (curve) that is dynamic in that it moves and changes its shape. The word snake is used to describe how the contour appears to slither like a snake as it moves. The work done by Kass et al is the foundation upon which the work done for this thesis is based.

The idea of a snake active contour proposed by Kass et al is an active contour model “using an energy-minimizing spline guided by external constraint forces and influenced by image forces that pull it toward features such as lines and edges. Snakes are active contour models: they lock onto nearby edges, localizing them accurately” [5]. A snake active contour is a parametric curve, C , defined within the image domain that dynamically evolves (reshapes itself) from its initial shape and location under the influence of forces defined within the curve (known as internal forces) and forces calculated from image (known as external forces) to finally settle on the boundary of an object it is placed in proximity to. The process of going from the initial curve to the final curve is cast as an energy

functional minimization problem by Kass et al. In the process of minimizing its energy, the curve is moved by the internal and external forces which cause the curve to be drawn to its minimum energy shape and location which turns out to be an object boundary. At this location the internal and external forces balance each other out, therefore stopping the snake's deformation.

Snake active contours have been used extensively for segmentation and more advanced methods have been developed such as geometric active contours [6] and active contours without edges [7]. Active contours have been used to segment and track structures ranging from macroscopic to microscopic in scale including the brain, arteries and chromosomes [4].

Due to the promising results that have been obtained with active contours in segmenting various types of objects, we decided to use them for the segmentation of the cell images obtained by the ODDT group. The images collected by the group consisted of co-registered monochrome image triplets consisting of a DIC (differential interference contrast) image made with transillumination, a fluorescent image taken with excitation and emission filters specific to FAD (flavin adenine dinucleotide) and a fluorescent image taken with excitation and emission filters specific to NADH (nicotinamide adenine dinucleotide). Our initial aim was to use all three images in the segmentation process because each image contained different type of information about the cells. However, we ended up just using the NADH images because the DIC images did not provide much useful information and the FAD images were too noisy compared to the NADH images.

Initially, the snake active contour method presented by Kass et al was used to segment the human epidermal cells in the NADH images. Unfortunately, the method did not give good results if the contour was not initialized very close to cell of interest. To overcome this limitation, reading the active contour literature and experimenting with other methods, led to charged active contours based on electrostatics (charge active contour) by Yang et al [8]. By combining the energy minimization model from the snake active contour and forces based on electrostatics dynamics suggested by Yang et al [8], we were able to obtain satisfactory results segmenting the nucleus and cell wall of the cells in the NADH images.



The outline of the paper is as follows. The following chapter presents some basic principles of image processing and introduces traditional edge-based segmentation methods which are referred to in later chapters. Chapter 3 presents the mathematical foundations of snake active contours and charged active contours. Chapter 4 describes the implementation details of the snake active contour method and the combined snake and charged active contour method. The results obtained from both methods are presented in Chapter 5. The conclusion and future work are discussed in Chapter 6.

Please note that the technical name for the method proposed by Kass et al is *snakes: active contour model*. However, during the course of this paper as it is in the published literature words such as snakes, active contour, snake active contour, classical snake, contour and curve will be used interchangeable to refer to *snakes: active contour model*.

CHAPTER 2: TRADITIONAL SEGMENTATION METHODS

2.1 Image Processing Basics

In digital image processing, a gray scale (monochrome) image is defined as a discrete 2-dimensional function $f(x, y)$, composed of a finite number of elements known as pixels. Each pixel has spatial coordinates given by (x, y) . The value of the function f at any pair of coordinates (pixel location) is proportional to the brightness (intensity of light) of the image at that location. Since we are dealing with discrete monochrome images, there are a finite number of brightness levels. Each brightness level is known as a gray level. The images used for this thesis have 65,536 levels. A value of 0 is black while a value of 65,535 is white. The values between those two are shades of gray, with higher values being lighter shades of gray than lower values.

An edge is a change in gray levels between neighboring pixels in an image. The rate of change can be rapid or slow resulting in a strong or weak edge. Locating edges in an image is usually done by applying edge detectors and/or edge enhancers to the image.

When an edge detector is applied on an image the result is a binary image (An image that has only two possible gray level values for each pixel.) known as the edge map. The edge map allows one to distinguish between edge and non-edge pixels. For example, edge pixels will be white while non-edge pixels will be black. Edge enhancers on the other hand, can not distinguish between edge and non-edge pixels. They just increase the contrast between edge pixels and non-edge pixels in an image. The following section will present an edge enhancer, the

gradient, and two edge detectors, thresholding and canny which are used in implementing the combined snake and charged active contour.

2.2 Gradient

The gradient is a mathematical operator from vector calculus. The gradient of a scalar field (a function) is a vector field where each vector points in the direction of greatest increase of the function. Applied to an image, the gradient gives the directions and rates of change of gray levels from pixel to pixel. The gradient at each image pixel is a vector whose components are calculated by the derivatives of the image in the direction of the coordinate axes. The gradient of an image $I(x, y)$ at location (x, y) is defined by the vector:

$$\nabla I = \frac{\partial I}{\partial x} + \frac{\partial I}{\partial y} = \begin{bmatrix} G_x \\ G_y \end{bmatrix} \quad \text{💬} \quad (2.1)$$

where G_x and G_y are the partial derivatives of the image with respect to the horizontal and vertical directions. The magnitude and direction of the gradient are given by:

$$mag(\nabla I) = [G_x^2 + G_y^2]^{1/2} \quad (2.2)$$

$$angle(\nabla I) = \arctan\left(\frac{G_y}{G_x}\right) \quad (2.3)$$

The gradient of an image as indicated by (2.1) is computed by taking the partial derivatives of the image in the horizontal and vertical directions. This is accomplished by convolving two spatial filters (also known as masks), that implement first order derivatives, with the image in the horizontal and vertical

directions to get two images G_x (horizontal edge image) and G_y (vertical edge image). There are a number of such masks such as the Roberts and Sobel masks [3] but the simplest ones are the following:

$$\begin{bmatrix} -1 & 0 & +1 \end{bmatrix}$$

Figure 1: Horizontal Gradient Mask

$$\begin{bmatrix} -1 & 0 & +1 \end{bmatrix}^T$$

Figure 2: Vertical Gradient Mask

The following figures illustrate the result of taking the gradient of a simple image.



Figure 3: Test Image 1



Figure 4: Gradient Image of Test Image 1 - obtained using Eqn. 2.2

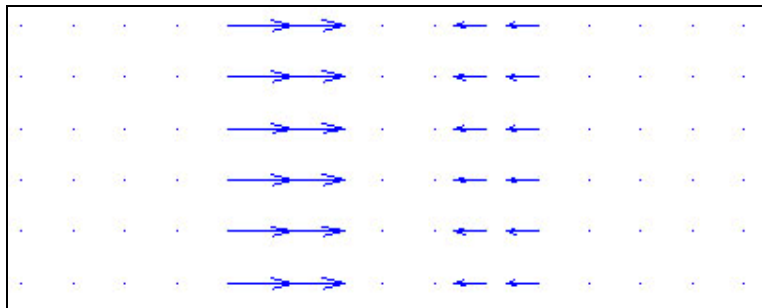


Figure 5: Zoom on Vector Field produces by taking the gradient of Figure 3

Analyzing figures 3 through 5, two important observations can be made. First, in homogeneous regions the gradient is zero (black). This indicates that there is no change in the gray levels of neighboring pixels. Second, at an edge, in the gradient image, the magnitude of the gradient is proportional to the rate of change in gray level. This is seen in figure 5 where the vectors on the left, indicating the transition from black to white in figure 3 have a much large magnitude than the vectors on the right that indicate a transition from gray to white. Another thing to note is that in the gradient image the color of an edge depends on how strong (rate of pixel gray level change) an edge is. The stronger an edge, the whiter the pixels at that location will be in the gradient image.

2.3 Thresholding

Thresholding is a simple image segmentation technique. The basic idea is to assume that the image is comprised to two types (or classes) of pixels: background and object pixels, each with a different gray level. Thresholding is performed by choosing a threshold value from the gray scale range of the image and following a rule that marks pixels above or under threshold differently. For example, using a 256 gray scale range, pixels that fall below the threshold are labeled with gray level “0” (black) while those above the threshold are labeled with gray level “255” (white). The result of thresholding an image in such a manner is a binary image. Here is an example of a thresholding rule:

$$I_T(x,y) = \begin{cases} 0 & I(x,y) \leq T \\ 255 & I(x,y) > T \end{cases} \quad T = \text{Threshold value} \quad (2.4)$$

$I(x, y)$ represents the original image and $I_T(x, y)$ is the image after thresholding. Image thresholding can also be performed using multiples threshold values, which will separate the pixels into the desired number of classes. Figures 6 through 9 illustrate the results of taking the threshold on Test Image 2 shown in Figure 6.

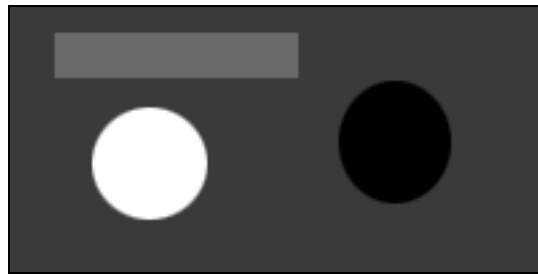


Figure 6: Test Image 2

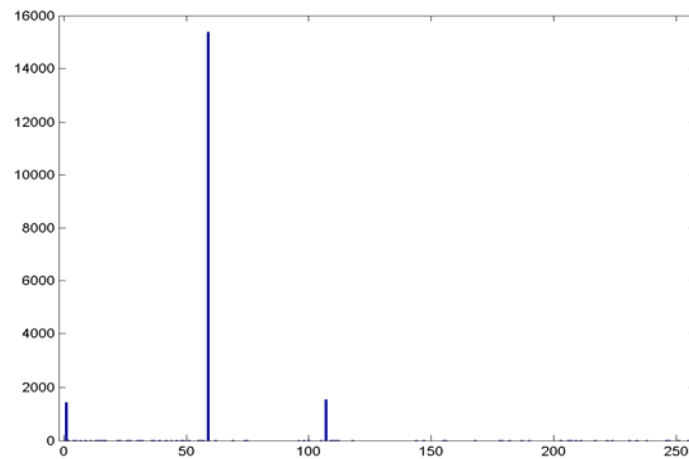


Figure 7: Histogram of Test Image 2



Figure 8: Test Image 2 after Thresholding with $T = 75$



Figure 9: Test Image 2 after Thresholding with $T = 150$

Depending on the image one is working with finding the right threshold value that properly segments the image for the application at hand can be a very a daunting task. This is especially true if the image does not have a histogram that indicates clear demarcations of the pixel gray levels in the image.

2.4 Canny Operator

The canny operator is one of the most well known and used edge detection methods in image processing. It was developed by John Canny in 1983 for his Masters thesis at MIT [9].

The canny operator is a multi-step process that incorporates image thresholding and image gradient to detect edges. First, the image of interest is smoothed to reduce noise. Second, the gradient of the image is taken. This is

done to obtain regions with high spatial derivatives which indicate the presence of edges. Third, the edges in the gradient image are thinned (made one pixel thick). This is accomplished by suppressing (setting to zero by a process known as non-maxima suppression) pixels that do not have the maximum gray level amongst their surrounding pixels. Forth, a thresholding technique referred to as hysteresis is used to clean up the thinned gradient image. Hysteresis works by using two threshold values. If the magnitude of a pixel is above the high threshold, it is labeled as an edge (set to gray level 255). If it is below the low threshold it set to zero (labeled as a non-edge). If a pixel happens to fall between the two thresholds, it is set to zero unless it is connected to a pixel that is above the high threshold (this removes single edge points which cause broken edges). The result of these four steps is a binary image indicating the edges in the image. Figure 10 shows the results of apply the canny operator on Test Image 2.



Figure 10: Result of Canny Operator Applied to Test Image 2

CHAPTER 3: MATHEMATICAL BACKGROUD

3.1 Introduction

In their survey of deformable models in medical image analysis [4], McInerney and Terzopoulos provide the following mathematical formulation of deformable models:

The mathematical foundations of deformable models represent the confluence of geometry, physics, and approximation theory. Geometry serves to represent object shape, physics imposes constraints on how the shape may vary over space and time, and optimal approximation theory provides the formal underpinnings of mechanisms for fitting the models to measured data.

The name “deformable models” stems primarily from the use of elasticity theory at the physical level, generally within a **Lagrangian dynamics** setting. The physical interpretation views deformable models as elastic bodies (e.g. rubber band) which respond naturally to applied forces and constraints. Typically, deformation energy functions defined in terms of the geometric degrees of freedom are associated with the deformable model. The energy grows monotonically as the model deforms away from a specified natural or “rest shape” and often includes terms that constrain the smoothness or symmetry of the model. In the Lagrangian setting, the deformation energy gives rise to elastic forces internal to the model. Taking a physics-based view of classical optimal approximation, external potential energy functions are defined in terms of the data (the image with the object to be segmented) of interest to which the model is to be fitted. These potential energies give rise to external forces which deform the model such that it fits the data.

3.2 Snake Active Contour

A snake is an energy minimizing parametric curve, C , represented by the vector $\mathbf{v}(s) = (x(s), y(s))$, where x and y are coordinate functions of s , the normalized arc length. $s \in [0, 1]$ is the parametric domain. For the purpose of this thesis we will be dealing exclusively with closed curves so $C(0) = C(1)$.

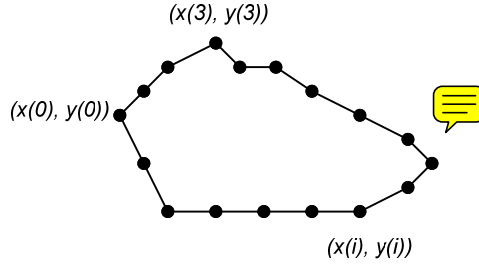


Figure 11: Parametric Curve with Control Points $\mathbf{v}(s) = (x(s), y(s))$

To conform to the boundary of an object it is placed in proximity to, a snake works by minimizing an associated energy functional. The energy functional associated with the snake can be viewed as the representation of the energy of the snake and the final snake corresponds to the minimum of this energy [4]. A snake conforms to the boundary of an object by deforming its shape and moving through the spatial domain of the image until it reaches a location (theoretically the object's boundary) where its energy functional E_{snake}^* is at a minimum. The energy functional is defined as follows:

$$E_{snake}^* = \int_0^1 E_{snake}(\mathbf{v}(s)) ds \quad (3.1)$$

$$E_{snake}^* = \int_0^1 E_{int}(\mathbf{v}(s)) + E_{ext}(\mathbf{v}(s)) ds \quad (3.2)$$

$$E_{ext} = E_{image}(\mathbf{v}(s)) + E_{con}(\mathbf{v}(s)) \quad (3.3)$$

$$E_{snake}^* = \int_0^1 E_{int}(\mathbf{v}(s)) + E_{image}(\mathbf{v}(s)) + E_{con}(\mathbf{v}(s)) ds \quad (3.4)$$

where E_{int} , E_{ext} , E_{image} and E_{con} respectively denote internal energy, external energy, external image energy and external constraint energy [5]. The internal energy, E_{int} , is calculated based on the shape and location of the snake and serves to preserve the continuity and smoothness of the snake. The external energy term, E_{ext} , is composed of two terms: the external image energy term and the external constraint energy term. The external image energy, E_{image} , is calculated using image information, typically the negative magnitude of the gradient of the image, and is used to drive the snake towards image features like lines, edge and subjective contours [5]. The external constraint energy, E_{con} , is an optional term that is responsible for forcing the snake away or towards any particular feature in the image. This optional term is defined by a user or some other higher level process. The expanded general form of the energy functional without the optional constraint energy term is:

$$E_{snake}^* = \int_0^1 \frac{1}{2} \alpha(s) \left| \frac{d\mathbf{v}}{ds} \right|^2 + \frac{1}{2} \beta(s) \left| \frac{d^2\mathbf{v}}{d^2s} \right|^2 + E_{ext}(\mathbf{v}(s)) ds \quad (3.5)$$

where $\alpha(s)$ and $\beta(s)$ are non-negative weighting parameters that control the snake's tension (elasticity) and rigidity (inability to bend). In most applications and for this thesis they are treated as constants [5]. From calculus of variations, the snake that minimizes the energy functional must satisfy the following Euler equation [4]:

$$-\frac{\partial}{\partial s}\left(\alpha(s)\frac{\partial \mathbf{v}(s)}{\partial s}\right) + \frac{\partial^2}{\partial s^2}\left(\beta(s)\frac{\partial^2 \mathbf{v}(s)}{\partial s^2}\right) + \nabla E_{ext} = 0 \quad (3.6)$$

In compact form:

$$\alpha(s)\mathbf{v}''(s) - \beta(s)\mathbf{v}''''(s) - \nabla E_{ext} = 0 \quad (3.7)$$

The above equation can be viewed as a force balance equation:

$$F_{int} + F_{ext} = 0 \quad (3.8)$$

where $F_{int} = \alpha(s)\mathbf{v}''(s) - \beta(s)\mathbf{v}''''(s)$ and $F_{ext} = -\nabla E_{ext}$. F_{int} and F_{ext} denote internal force and external force respectively. The internal force discourages stretching and bending while the external force pulls the snake towards the desired image edges [10]. Using these force terms, the deformation process of the snake can be viewed as an interaction of forces. The deformation process stops when the forces balance each other out $F_{int} = -F_{ext}$, ~~i.e. when the snake is on the boundary.~~

In order to find the solution to (3.7), the snake is treated as a function of time t as well as s i.e. $\mathbf{v}(s, t)$ [10]. The partial derivative of \mathbf{v} with respect to t is then set equal to the left hand side of (3.7):

$$\mathbf{v}_t(s, t) = \alpha\mathbf{v}''(s, t) - \beta\mathbf{v}''''(s, t) - \nabla E_{ext} \quad (3.9)$$

When the solution $\mathbf{v}(s, t)$ stabilizes, the term $\mathbf{v}_t(s, t)$ goes to zero and we obtain the solution $\mathbf{v}(s, t_{final})$ to equation (3.7).

3.2.1 Internal Energy and Force

$$E_{\text{int}} = \frac{1}{2} \alpha \left| \frac{d\mathbf{v}}{ds} \right|^2 + \frac{1}{2} \beta \left| \frac{d^2\mathbf{v}}{d^2s} \right|^2 \quad (3.10)$$

The internal energy, E_{int} , and internal force are functions of the contour and are composed of two terms. The first term makes the snake act like a membrane to resist stretching thus enabling the snake to be continuous. The second term causes the snake to act like a thin-plate to resist bending making the snake smooth. The coefficients α and β , known as the tension and rigidity parameters are scaling factors that control the relative influence of the membrane and thin-plate terms. α determines the extent to which the snake can stretch at a point s on the snake while β determines the extent to which the snake can bend at a point s . By increasing the value of α one increases the “tension” in a snake thereby reducing the length of the snake. On the other hand, increasing the value of β increases the bending “rigidity” of the snake and makes the snake smoother and less flexible [4]. Setting β to zero at a point s on the snake allows the snake to become second-order discontinuous and develop a corner [5].

3.2.2 External Energy and Force

As was previously mentioned, E_{ext} , the external energy (without the optional external constraint energy term), calculated from the image that contains the object one is trying to segment, is responsible for pushing the snake towards an object’s boundary. This is accomplished by using the gradient image. If \mathbf{I} is the

original image containing the object to be segmented, $\nabla \mathbf{I}$, the gradient image will have high gray levels at pixels located at edges in \mathbf{I} . By setting E_{ext} as follows:

$$E_{ext}(\mathbf{v}(s)) = -|\nabla \mathbf{I}|^2 \quad (3.11)$$

near an edge the energy of the snake will drop drastically. As a result, the energy minimizing nature of the snake will push the snake towards an edge and hold it there.



3.3 Charged Active Contour

The charged active contour is an active contour model based on charged particles (electrons and protons), electrostatics and particle movement. As in the snake active contour model, a contour is used to locate the boundary of an object. This is accomplished by modeling the curve as a set of connected positive charged particles and the edge pixels in the image as fixed negative charges. This presence of charges creates an “electrostatic field” which moves the positive charges (the contour) to the negative charges (the object boundary). The force exerted by the electrostatic field is composed of two forces: a boundary attraction force which attracts the protons to the electrons and a boundary competition force which causes the protons to repel each other.

3.3.1 Boundary Attraction Force Field

The construction of the boundary attraction force is based on the location of boundary pixels in the image of interest and the strength (gray level) of the pixels. The boundary pixels obtained from an edge enhancer or edge detector are

treated as fixed negative charges with magnitude proportional to their edge strength [8]. Let N denote the number of negative charges at locations $\mathbf{r}_1, \mathbf{r}_2 \dots \mathbf{r}_N$ across the edge map and let $f(\mathbf{r}_i)$ denote the magnitude of the edge map at each of these locations. Using the above notation, we can assign a charge q_i to each edge pixel at location \mathbf{r}_i as follows: $q_i = -f(\mathbf{r}_i) < 0$. The electrostatic field \mathbf{E}_A (attractive electrostatic field) generated by these negative charges can be computed according to Coulomb's Law as [8]:

$$\mathbf{E}_A(\mathbf{x}) = \sum_{i=1}^N \frac{q_i}{4\pi\epsilon_0} \frac{\mathbf{x} - \mathbf{r}_i}{|\mathbf{x} - \mathbf{r}_i|^3}, \quad \mathbf{x} \in \mathbf{X} \quad (3.12)$$

where \mathbf{X} is the set of all possible locations in the 2D domain of the image.

Expanding (3.12) we obtain:

$$\left[\sum_{i=1}^N \frac{q_i}{4\pi\epsilon_0} \frac{\mathbf{x}_x - \mathbf{r}_{i,x}}{\left(\sqrt{(\mathbf{x}_x - \mathbf{r}_{i,x})^2 + (\mathbf{x}_y - \mathbf{r}_{i,y})^2} \right)^3} \right] \hat{\mathbf{i}} + \left[\sum_{i=1}^N \frac{q_i}{4\pi\epsilon_0} \frac{\mathbf{x}_y - \mathbf{r}_{i,y}}{\left(\sqrt{(\mathbf{x}_x - \mathbf{r}_{i,x})^2 + (\mathbf{x}_y - \mathbf{r}_{i,y})^2} \right)^3} \right] \hat{\mathbf{j}}$$

This electrostatic vector field is a bi-directional force field pointing towards the negative fixed charges, i.e. the edges.

As previously mentioned, the active contour can be considered as a set of connected positive charged particles. Let M denote the number of positive charges at locations $\mathbf{s}_1, \mathbf{s}_2 \dots \mathbf{s}_M$ each with a charge p_j , where $p_j > 0$. The attractive electrostatic force felt by the positive charges at locations $\mathbf{s}_1, \mathbf{s}_2 \dots \mathbf{s}_M$ on the contour is:

$$\mathbf{F}_A(\mathbf{s}_j) = p_j \mathbf{E}_A(\mathbf{s}_j), \quad \mathbf{s}_j \in \mathbf{X} \quad (3.13)$$

In this thesis, a constant unit positive p_j charge is assigned to all contour points. Since the contour and the fixed charge are of opposite polarity, from electrostatic theory, the electrostatic boundary attraction force will push the contour towards object boundaries.

3.3.2 Boundary Competition Force Field

The boundary competition force causes the protons on the contour to repel each other. This is necessary so that free positive charges on the contour do not approach object boundaries that are already occupied by other positive charges of the contour. This competition force is the result of an electrostatic field that is continuously adapting as the contour evolves and reaches boundaries [8]. The electrostatic competition force field is defined such that: (a) Contour points (positive charges) that are on object boundaries endow the most to the field with contributions proportional to the edge strength of the edge pixels they are on. (b) The force upon a contour point due to the electrostatic competition field is proportional to the inverted strength of the edge covered by contour point [8]. This results in contour points in homogeneous regions feeling the most competition force while those on top of strong edges feel very little of the force. This ensures that contour points that have detected boundaries stay there but push away nearby contour points from the same boundary point. Condition (a) is accomplished by weighting the contour charges with the edge function, $p'_j = -f(s_j) p_j$. The resulting electrostatic competition field is composed of vectors that

point away from the edges already occupied by contour points [8]. Using Coulomb's Law the competition field is:

$$\mathbf{E}_C(\mathbf{x}) = \sum_{j=1}^M \frac{p'_j}{4\pi\epsilon_0} \frac{\mathbf{x} - \mathbf{s}_j}{|\mathbf{x} - \mathbf{s}_j|^3} = \sum_{j=1}^M \frac{f(\mathbf{s}_j)p_j}{4\pi\epsilon_0} \frac{\mathbf{x} - \mathbf{s}_j}{|\mathbf{x} - \mathbf{s}_j|^3}, \quad \mathbf{x} \in \mathbf{X} \quad (3.14)$$

The competition force, \mathbf{F}_C , described in (b) which prevents contour points from approaching the same boundary location is generated by weighting contour charges with an edge stopping function, i.e. $g(\cdot) = 1 - f(\cdot)$.

$$\mathbf{F}_C(\mathbf{s}_j) = g(\mathbf{s}_j)p_j\mathbf{E}_C(\mathbf{s}_j), \quad \mathbf{s}_j \in \mathbf{X} \quad (3.15)$$

The following is an example from [8] illustrating the effect of the competition force:

Consider positive point charges p_a and p_b on the active contour at positions \mathbf{s}_a and \mathbf{s}_b . If these two points are both in homogenous regions, $\mathbf{E}_C(\mathbf{s}_a)$ and $\mathbf{E}_C(\mathbf{s}_b)$ are small, and they exert little competition force upon each other (and on other snake points). However, both of them are strongly repelled by any other points that have already reached boundaries. When one of this pair, say p_a , reaches a boundary, it (along with all other snake points on object boundaries) will alter the electrostatic field according to (3.14), with its contribution to the field being proportional to its edge strength $f(\mathbf{s}_a)$. The impact of this electrostatic field on p_a itself is however minimized since the force $\mathbf{F}_C(\mathbf{s}_a)$ is weighted by $g(\mathbf{s}_a)$ (in (3.15)), i.e. the stopping function prevents it from being pushed away from the boundary. The snake point p_b on the other hand provides little contribution to this field, but will be most affected by the competition force $\mathbf{F}_C(\mathbf{s}_b)$ due to the large value of $g(\mathbf{s}_b)$ in the homogeneous region. When both snake points reach a boundary, they both contribute to the electrostatic field but have barely any influence on each other.

3.3.3 Joint Electrostatic Force

By combining the attraction force and the competition force we obtain the joint electrostatic force \mathbf{J} , the net force on the contour, which is constantly been updated as contour points move:

$$\begin{aligned} J(s_j) &= p_j [\lambda E_A(s_j) + (1 - \lambda) g(s_j) p_j E_C(s_j)] \\ &= \lambda F_A(s_j) + (1 - \lambda) F_C(s_j) \end{aligned} \tag{3.16}$$

Lambda (λ) is a real positive constant that balances the contributions between the boundary attraction force and the boundary competition force.

CHAPTER 4: IMPLEMENTING ACTIVE CONTOURS

4.1 Implementation of Snake Active Contour

In order to numerically compute the minimum energy contour that solves (3.5) we must discretize the energy functional E_{snake}^* and the contour C . This is done by using numerical methods and treating the snake as a contour consisting of n vertices (control points) connected by straight lines. Integrals become summations and derivatives become finite differences. Putting this together using (3.1) through (3.5) and representing a point on the contour as $\mathbf{v}_i = (x_i, y_i)$ we obtain:

$$\begin{aligned}
 E_{snake}^* &= \int_0^1 E_{int}(\mathbf{v}(s)) + E_{ext}(\mathbf{v}(s)) ds \\
 E_{snake}^* &= \int_0^1 \frac{1}{2} \alpha(s) \left| \frac{d\mathbf{v}}{ds} \right|^2 + \frac{1}{2} \beta(s) \left| \frac{d^2\mathbf{v}}{d^2s} \right|^2 + E_{ext}(\mathbf{v}(s)) ds \\
 \left| \frac{d\mathbf{v}}{ds} \right|^2 &\approx |\mathbf{v}_i - \mathbf{v}_{i-1}|^2 = (x_i - x_{i-1})^2 + (y_i - y_{i-1})^2 \\
 \left| \frac{d^2\mathbf{v}}{d^2s} \right|^2 &\approx |\mathbf{v}_{i-1} - 2\mathbf{v}_i + \mathbf{v}_{i+1}|^2 = (x_{i-1} - 2x_i + x_{i+1})^2 + (y_{i-1} - 2y_i + y_{i+1})^2 \\
 E_{snake}^* &= \sum_{i=1}^n [E_{int}(\mathbf{v}_i) + E_{ext}(\mathbf{v}_i)] \\
 E_{snake}^* &= \sum_{i=1}^n \alpha |\mathbf{v}_i - \mathbf{v}_{i-1}|^2 + \beta |\mathbf{v}_{i-1} - 2\mathbf{v}_i + \mathbf{v}_{i+1}|^2 + -|\nabla I| \quad (4.1)
 \end{aligned}$$

Since we are dealing with closed contours the first and last vertices are at the same location, therefore $\mathbf{v}_{first} = \mathbf{v}_{last}$. From [5] and (3.7), the corresponding Euler equation to be used for the energy minimization of the active contour is:

$$\begin{aligned} & \alpha(x_i - x_{i-1}) - \alpha(x_{i+1} - x_i) \\ & + \beta[x_{i-2} - 2x_{i-1} + x_i] - 2\beta[x_{i-1} - 2x_i + x_{i+1}] + \beta[x_i - 2x_{i+1} + x_{i+2}] + \frac{\nabla E_{ext}}{\partial x} = 0 \end{aligned} \quad (4.2a)$$

$$\begin{aligned} & \alpha(y_i - y_{i-1}) - \alpha(y_{i+1} - y_i) \\ & + \beta[y_{i-2} - 2y_{i-1} + y_i] - 2\beta[y_{i-1} - 2y_i + y_{i+1}] + \beta[y_i - 2y_{i+1} + y_{i+2}] + \frac{\nabla E_{ext}}{\partial y} = 0 \end{aligned} \quad (4.2b)$$

Combining (4.2a) and (4.2b) we obtain:

$$\begin{aligned} & \alpha(\mathbf{v}_i - \mathbf{v}_{i-1}) - \alpha(\mathbf{v}_{i+1} - \mathbf{v}_i) \\ & + \beta[\mathbf{v}_{i-2} - 2\mathbf{v}_{i-1} + \mathbf{v}_i] - 2\beta[\mathbf{v}_{i-1} - 2\mathbf{v}_i + \mathbf{v}_{i+1}] + \beta[\mathbf{v}_i - 2\mathbf{v}_{i+1} + \mathbf{v}_{i+2}] + \frac{\nabla E_{ext}}{\partial y} = 0 \end{aligned} \quad (4.2c)$$

Writing (4.2c) in matrix form we obtain the following pair of equations:

$$\mathbf{A}\mathbf{x} + \frac{\partial E_{ext}}{\partial x}(x, y) = 0 \quad (4.3)$$

$$\mathbf{A}\mathbf{y} + \frac{\partial E_{ext}}{\partial y}(x, y) = 0 \quad (4.4)$$

\mathbf{A} is a pentadiagonal banded matrix of size $(n \times n)$ where n is the number of vertices in the contour. As a simple example, let us assume we have a contour with $n = 6$ as illustrated in figure 11. Each row of \mathbf{A} , m , contains the coefficients of the expanded version of (4.2c) (without the E_{ext} term) for $i = m$.

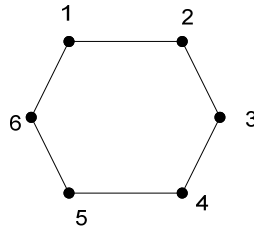


Figure 12: Snake with $N=6$ vertices

$$\mathbf{A} = \begin{bmatrix} 2\alpha + 6\beta & -\alpha - 4\beta & \beta & 0 & \beta & -\alpha - 4\beta \\ -\alpha - 4\beta & 2\alpha + 6\beta & -\alpha - 4\beta & \beta & 0 & \beta \\ \beta & -\alpha - 4\beta & 2\alpha + 6\beta & -\alpha - 4\beta & \beta & 0 \\ 0 & \beta & -\alpha - 4\beta & 2\alpha + 6\beta & -\alpha - 4\beta & \beta \\ \beta & 0 & \beta & -\alpha - 4\beta & 2\alpha + 6\beta & -\alpha - 4\beta \\ -\alpha - 4\beta & \beta & 0 & \beta & -\alpha - 4\beta & 2\alpha + 6\beta \end{bmatrix} \quad (4.5)$$

To solve (4.3) and (4.4), the right hand sides of the equations are set equal to the product of a step size and the negative time derivatives of the left-hand sides [5].

$$\mathbf{A}\mathbf{x}_t + \frac{\partial E_{ext}(x_{t-1}, y_{t-1})}{\partial x} = -\gamma(\mathbf{x}_t - \mathbf{x}_{t-1}) \quad (4.6)$$

$$\mathbf{A}\mathbf{y}_t + \frac{\partial E_{ext}(x_{t-1}, y_{t-1})}{\partial y} = -\gamma(\mathbf{y}_t - \mathbf{y}_{t-1}) \quad (4.7)$$

In the above equations, gamma (γ) is the step size and the subscript t is the iteration step. At equilibrium, the time derivative goes to zero and we end up with solutions to (4.6) and (4.7). The solutions to (4.6) and (4.7), \mathbf{x} and \mathbf{y} , are obtained iteratively by matrix inversion:

$$\mathbf{x}_t = (\mathbf{A} + \gamma \mathbf{I})^{-1} \left(\gamma \mathbf{x}_{t-1} - \frac{\partial E_{ext}(x_{t-1}, y_{t-1})}{\partial x} \right) \quad (4.8)$$

$$\mathbf{y}_t = (\mathbf{A} + \gamma \mathbf{I})^{-1} \left(\gamma \mathbf{y}_{t-1} - \frac{\partial E_{ext}(x_{t-1}, y_{t-1})}{\partial y} \right) \quad (4.9)$$

where \mathbf{I} is an $n \times n$ identity matrix.

4.2 Combined Snake and Charged Active Contour

Implementing the combined snake and charge active follows the exact same steps outlined in section 4.1. The only difference it that instead of using $E_{ext} = -|\nabla I|$, $E_{ext} = \mathbf{J}$, the joint electrostatic force developed in section 3.3.3.

4.2.1 Segmenting the NADH Cell Images

We segmented cells in the NADH images by implementing the combined snake and charged active contour method (abbreviated as CSCAC). The implementation was carried out using MATLAB.

To be able to use CSCAC, one must be able to clearly distinguish between edge and non edge pixels so that one can assign negative charges to the edge pixels. The NADH images had non-uniform illumination and contained a lot of noise which made it practically impossible to distinguish between the edges of cells and the rest of the image. To overcome these drawbacks adaptive thresholding was applied to the NADH images. Adaptive thresholding refers to a variety of thresholding techniques which threshold an image by breaking it into sub-images and then use a different threshold on each sub-image. We performed adaptive thresholding by using 2D convolution to obtain an average image of the NADH image, subtracted the average image from the NADH image and then threshold the resulting image. The adaptive thresholding we used was not able to completely detect all the edges of every single cell in the NADH images but managed to do so for a good number of the cells.

The following is the simple pseudo-code of the algorithm implementing the cell segmentation.

1. Load NADH image.
2. Apply adaptive thresholding on the image.
3. Use the canny operator on the thresholded image to obtain an edge map.
4. User clicks in the center of the nucleus of the cell they want segmented.
5. Using the edge map, use CSCAC to find the boundary of the nucleus.
6. Once the boundary of the nucleus is found, remove the pixels in the edge map that belong to the boundary of the nucleus.
7. Using the new edge map, use CSCAC to find the boundary of the cell wall.



CHAPTER 5: RESULTS

This chapter presents the results of using the CSCAC method on NADH images. The original NADH images are quite large with a size of 800 x 600; therefore the images are cropped to just the cell one is interested in segmenting. Figures 13 through 18 show the results of the CSCAC on six different cells. In addition to the original and segmented cell images, figure 18 also shows the adaptively thresholded image that is used in the segmentation process. Using a synthetic image, figure 20 illustrates the progression of a snake from its original location to its final location on the object's boundary.

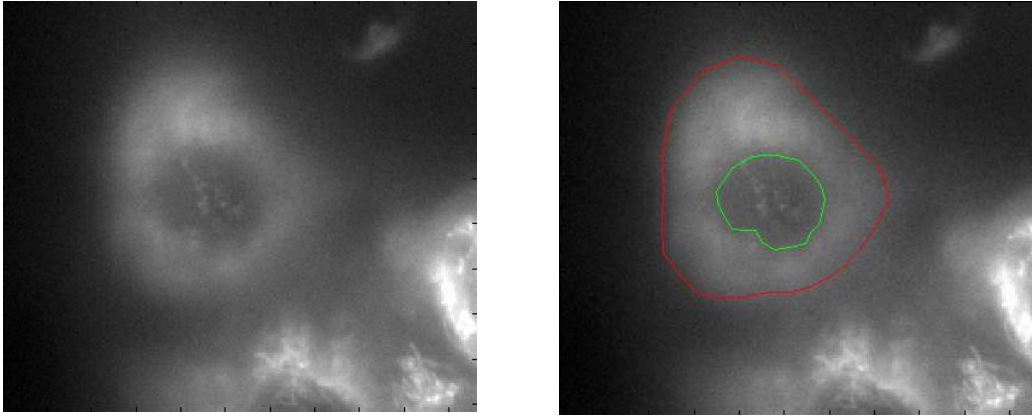


Figure 13: Result 1

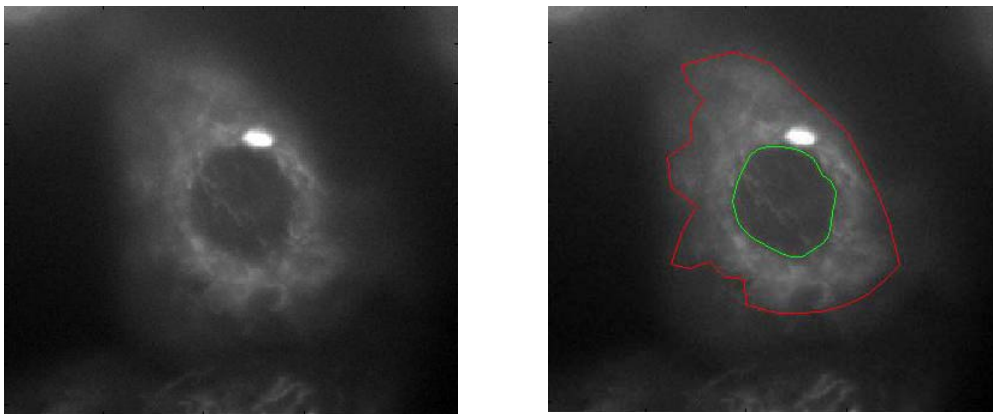


Figure 14: Result 2

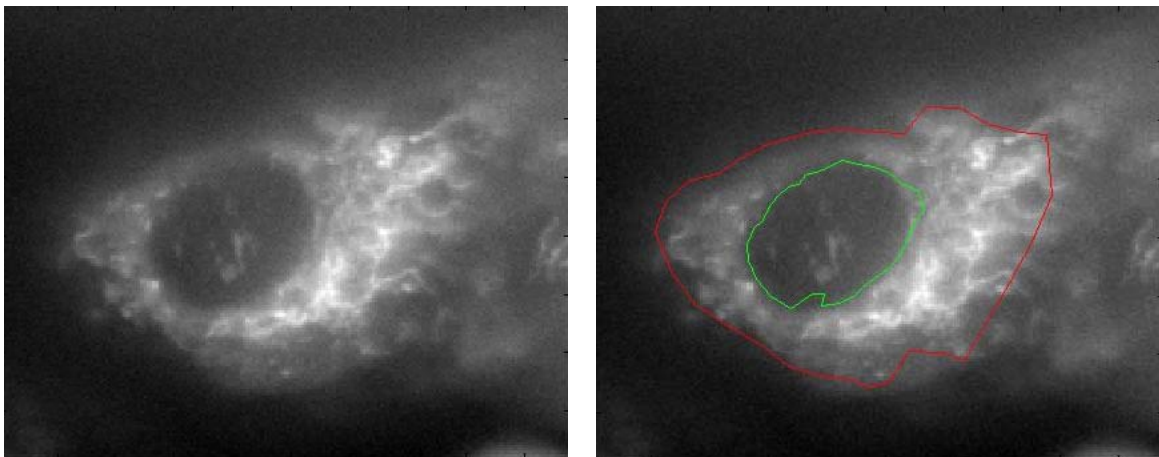


Figure 15: Result 3

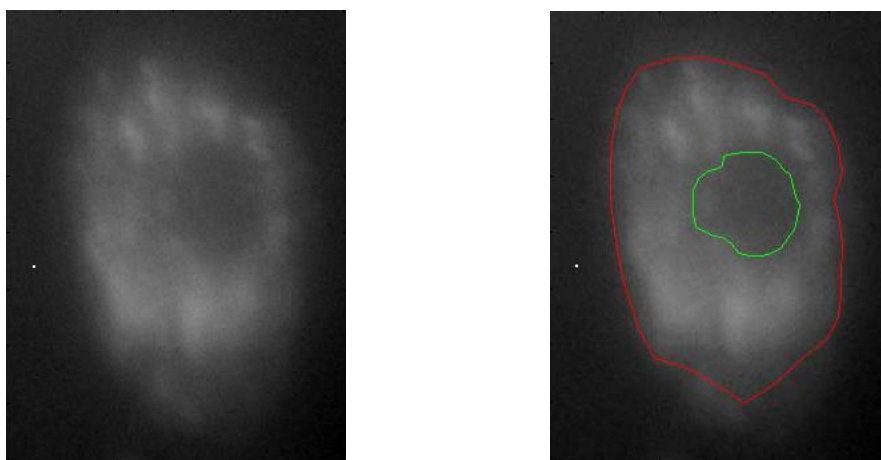


Figure 16: Result 4

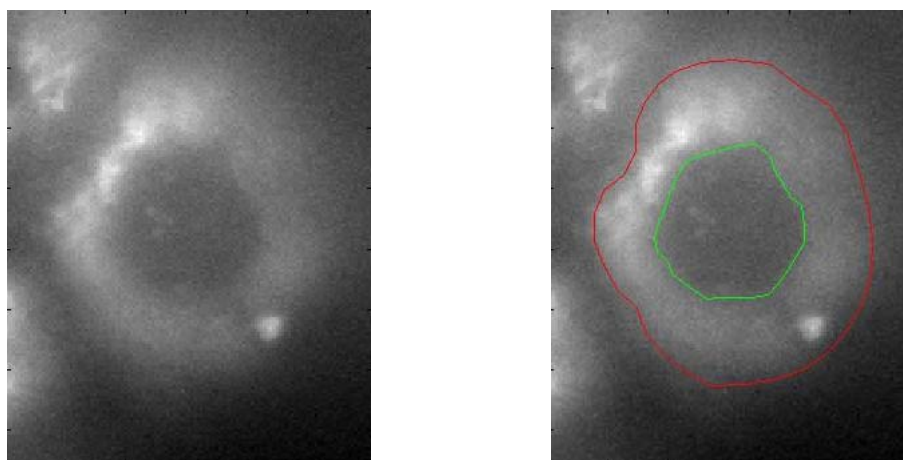


Figure 17: Result 5



Figure 18: Result 5

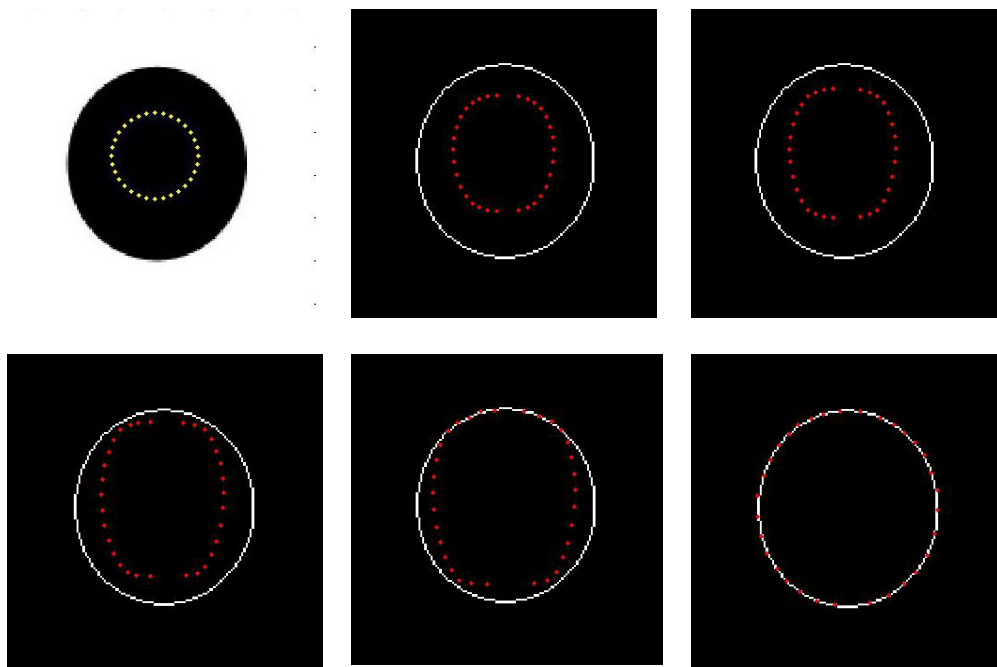


Figure 19: Snake Progression

Analyzing the figures above, the performance of CSCAC at segmenting the cells is remarkable considering that the cells do not have clearly demarcated nuclei or cell wall boundaries.

CHAPTER 6: CONCLUSION

In this thesis, we sought to address the problem of segmenting cell in NADH images. The images had a lot of negative attributes such as noise, non-uniform illumination and indistinguishable cell boundaries which had caused traditional segmentation methods to fail. To address this failure, we presented an extension of the work by Kass et al. on snake active contours to segment the cells. We found that by combining Kass's work with the concept of charged active contours developed by Yang et al. that we were successful at segmenting the cells.

Using the combined active contour methods to solve the segmentation problem was not a straight forward endeavor. Due to the absence of clear cell demarcations in the images, the actual NADH images were not directly used in the segmentation process. Instead the NADH images were preprocessed using adaptive thresholding to obtain a clearer image (in the sense that it had less noise and had clearer cell boundaries) which was used in the segmentation process.

Further work that can stem from this thesis is the development of a method that eliminates the NADH image drawbacks of noise and indistinct cell boundaries. Although adaptive thresholding gave good results it failed to work for all cells. Developing a technique that can overcome this will increase the range of cells that the combined snake and charged active contour can segment.

REFERENCES

- [1] American Cancer Society. *Cancer Facts & Figures 2007*. Atlanta: American Cancer Society; 2007
- [2] Tufts University – Optical Diagnostics for Diseased and Engineered Tissues Research Group. (2008, April). Development of Novel Optical Biomarkers for Early Cancer Detection. Available: <http://ase.tufts.edu/biomedical/research/georgakoudi/researchNovelOptical.asp>.
- [3] Gonzales, Rafael C. & Woods, Richard E. (2002), “Image Segmentation”, in *Digital Image Processing*, 2nd ed. Upper Saddle River: Prentice-Hall, 2002, pp. 567-635
- [4] McInerney, T., Terzopoulos, D. “Deformable models in medical image analysis: A survey,” *Medical Image Analysis*, 1 (2), pp. 91-108, 1996.
- [5] Kass, M., Witkin, A., Terzopoulos, D. “Snakes: Active contour models,” *International Journal of Computer Vision*, 1 (4), pp. 321-331, 1988.
- [6] Caselles, V., Kimmel, R., Sapiro, G. “Geodesic Active Contours,” *International Journal of Computer Vision*, 22 (1), pp. 61-79, 1997.
- [7] Chan, T.F., Vese, L.A. “Active contours without edges,” *IEEE Transactions on Image Processing*, 10 (2), pp. 266-277, 2001
- [8] Yang, R., Mirmehdi, M., Xie, X. "A charged active contour based on electrostatics," *Lecture Notes in Computer Science (including subseries Lecture Notes in Artificial Intelligence and Lecture Notes in Bioinformatics)*, 4179 LNCS, pp. 173-184, 2006
- [9] Nadernejad, E., Sharifzadeh, S., Hassanpour, H. “Edge Detection Techniques: Evaluations and Comparison,” *Applied Mathematical Sciences*, Vol. 2, no. 31, pp. 1507-1520, 2008
- [10] Xu, C., Prince, J.L. “Snakes, shapes, and gradient vector flow,” *IEEE Transactions on Image Processing*, 7 (3), pp. 359-369, 1998